Synthesis and characterization of bimetallic cobalt-lanthanide oxides for CO_2 methanation

Ricardo Alexandre Pinto da Silva (ist180801)
Instituto Superior Técnico

Abstract

The study of bimetallic Co-Ln oxides (Ln=La, Ce, Sm, Gd, Dy and Yb; Co/Ln=1) as catalysts for CO_2 hydrogenation was undertaken. The aerogels were obtained by the epoxide addition method, which demonstrated to be better when compared to the Pechini method. The aerogels were calcined at two different temperatures, 450 ºC and 900 ºC, which led to the formation of distinct oxide phases: oxychlorides in the case of calcination at 450 ° C with the structure Co_3O_4.3LnOCl (Ln = La, Sm, Gd and Dy) and perovskites $LnCoO_3$ (Ln = La, Sm, Gd and Dy) for calcination at 900°C. The exceptions, in both cases, were the Co-Ce (Co_3O_4.3CeO_2) and Co-Yb (2Co_3O_4.3Yb_2O_3) catalysts, which stabilized as sesquioxide phase. CO_2 hydrogenation studies showed that the catalytic performance depends on the calcination temperature, the addition rare earth and pre-reduction treatment. The best results were those obtained over bimetallic cobalt-cerium oxide, calcined at 900 ºC and pretreated under hydrogen (CO_2 conversion = 37%, CH_4 selectivity = 85.7%). The acid-base properties and the reducibility of the catalysts seem to be the main factors that influencing the catalytic performance of Co-Ln catalysts. The activity and the selectivity increase with catalysts basicity, showing an inverse dependence of the reduction temperature.

1 Introduction

The continuous consumption of fossil fuels has led to a considerable increase in the concentration of CO_2 in the atmosphere. Consequently, global climate changes caused by greenhouse gases, in particular CO_2, is a huge problem and a challenging one [1]. In order to overcome this problem, three strategies have been pointed out aiming the mitigation of CO_2 in the atmosphere: a) emission control, b) capture and storage and c) chemical conversion into value added products. Carbon storage is important for a rapid reduction of CO_2 levels, but it has major disadvantages, particularly the high cost, associated with its transport in liquefied state or the high risk due to CO_2 leakage from geological formations where was stored [1–3]. Therefore, the use of CO_2 in catalytic processes to generate value-added products is possibly the best strategy to follow. The CO_2 hydrogenation using H_2 from renewable energies is a very attractive route for the production of chemicals and fuels, which may constitute a viable alternative that not only reduces CO_2 emissions but also may respond to the growing demand and shortage of fossil fuels.

The main chemicals obtained through the CO_2 hydrogenation are alcohols and hydrocarbons, with special emphasis on methane that was the focus of this work. The catalysts generally used for this process are noble metals, nickel, cobalt, iron or copper metal catalysts supported on silica or alumina [4]. Transition metals have been extensively investigated as active catalysts for CO_2 hydrogenation. Noble metal-based catalysts, for example rhodium and ruthenium, are typically the most active for CO_2 methanation, producing almost exclusively CH_4, with CO_2 conversions of over 70% and selectivities close to 100% [5]. However, their high price makes them unattractive for commercial implementation.

Nickel-based catalysts are the most widely used and studied as an alternative for CO_2 methanation because they also present a high activity and selectivity to CH_4. Relatively to Fe- and Co-based catalysts, they are applied for the Fischer-Tropsch synthesis (FT) to produce long chain hydrocarbons, using synthesis gas (a mixture of CO and H_2) with a high ratio between its performance and cost. The similarity between CO and CO_2 hydrogenation reactions motivated researchers to study Fe and Co-based catalysts, which showed good performance in FT synthesis, also for CO_2 hydrogenation. However, under a mixture of CO_2 and H_2, cobalt-based catalysts are reasonably active and selective for methane rather than for the production of higher chain hydrocarbons[6,7]

The use of *f*-block elements as promoters has been studied, in particular with cerium. Recent studies show that the addition of cerium to a Fe-Zr-K catalyst promotes the reduction of the catalyst particles, increasing their basicity, favoring the dispersion of active Fe species and the activation of CO_2 [8]. Also, for cobalt catalysts, the addition of rare earths favour metal dispersion and the catalyst reducibility with a consequent increase in the C_{5+} hydrocarbon selectivity [9]. The addition of cerium to cobalt catalyst also increases the surface area and the decrease in particle size that promotes the catalytic activity [10].

In view of the above, bimetallic oxide aerogels were synthesized by the sol-gel methodology (Pechini method and epoxide addition method), combining cobalt and six lanthanides (lanthanum, cerium, samarium, gadolinium, dysprosium and ytterbium). Aerogels are porous materials with remarkable properties such as high functionality, high specific areas and high porosity, therefore being widely applied in the area of catalysis[11]. All catalysts were characterized by XRD, SEM/EDS, BET, H_2-TPR, CO_2-TPD and study of the dehydrogenation / dehydration of 2-propanol.

2 Experimental

2.1 *Catalyst preparation and characterization*

The bimetallic cobalt-lanthanide oxide catalysts were prepared by epoxide addition method. The bimetallic oxide catalysts (1:1 molar ratio between Co and Ln = La, Ce, Sm, Gd, Dy and Yb) were synthesized using chlorides of the respective metals as starting reagents, which were dissolved in absolute ethanol (Fischer Chemical,> 99.9%). The solution is stirred at room temperature until the chlorides are completely dissolved. Then propylene oxide is added, and the mixture is stirred for 5 minutes with the molar ratio of metals (M) to propylene oxide (OP) being 1:9. The solution is left at rest until complete gel formation. For example, for Co-Ce 1.1777 g (3 mmol) of $CeCl_3.7H_2O$ (Aldrich chemistry, 99%) and 0.7138 g (3mmol) of $CoCl_2.6H_2O$ (Alpha Aesar, 99%) were dissolved in 6.3 ml absolute ethanol and subsequently 3.86 ml (55 mmol) of propylene oxide (Acros organics, 99.5%) was added. The gel obtained was sealed in the preparation vessel and aged in ethanol for 48 hours at 50°C, then dried by the organic solvent sublimation method in 50%, 80% and 100% exchanging solvent (acetonitrile / ethanol (v / v)) for 24 hours at the same temperature. Then, the sample dried at 50 ºC. The product was grounded, and the particle size reduced to 200 mesh (75 µm). Finally, the samples were calcined at 450 and 900 °C during 2h at a heating rate of 1 °C/min. In the case of bimetallic Co-Ce oxide catalyst was also prepared by Pechini method[12]. The gel obtained was aged and dried, following the procedure used in epoxide addition method. This method was only applied in order to evaluate the best method for preparing the catalysts.

The crystalline structure of the samples was analysed by powder X-ray diffraction using a Bruker D8 advance diffractometer (Cu, kα monochromatic radiation, λ=1.5406 Å). The operational settings for all scans were voltage = 40 kV; current = 30 mA; 2θ scan range 19 – 81 º using a step size of 0.03 º at a scan speed of 0,06 º.s^{-1}. The particle size was determined by means of the Scherer's equation. Surface morphology was analysed by SEM using a FE-SEM JEOL JSM-6500F, operating at 15-20 keV and 80A. The surface chemical composition was determined by EDS using a B-U Bruker Quantax 400 EDS system Specific surface areas (BET method; single point relative pressure P/P_0=0.3, flow 20 mL/min using a mixture of 30% nitrogen in helium) were measured on a Micromeritics ChemSorb 2720 instrument. BET surface area of all catalysts are listed in Table 1.

Table 1 - Surface area of the aerogels as prepared and after calcination treatment.

Catalyst	**Surface area** ($m^2.g^{-1}$)		
	As prepared	**Calcined at 450°C**	**Calcined at 900°C**
Co-La	145.5±0.3	47.8±1.3	5.2±0.3
Co-Ce	160.1±0.7	64.9±1.3	6.8±0.2
Co-Sm	120.1±1.1	10.8±0.6	3.9±0.3
Co-Gd	130.8±0.9	31.9±1.1	5.4±0.2
Co-Dy	104.2±0.4	28.3±0.4	4.8±0.4
Co-Yb	133.4±4.3	40.5±1.7	9.8±0.5

The reducibility of the oxidized bimetallic oxides (H_2-TPR) were also performed on the Micromeritics ChemSorb 2720 instrument. The samples were placed in a specific Micromeritics quartz type U reactor and reduced under a 10% H_2 / argon mixture in the case of H_2-TPR at 10 ºC min^{-1}, from 20 to 1000 ºC using a total flow of 20 mL min^{-1}. Quantitative H_2-uptakes were evaluated by integration of the experimental H_2-TPR curves, based on previous calibration measurements with NiO powder (99.99995%, Aldrich). The acid-base properties of the catalysts were evaluated using CO_2 as probe (CO_2 –TPD) and studying its behavior on a model reaction: the dehydrogenation / dehydration of 2-propanol. Temperature-programmed desorption of CO_2 (CO_2-TPD) was carried out on a Micromeritics (ChemiSorb 2720- ChemiSoft TPx). At first CO_2 is adsorbed at a constant temperature (50 ° C) for 1 h and the catalyst is exposed to a large excess of carbon dioxide (pure, 20 mL / h flow). This is followed by flush with pure helium (20 mL / min; 1h) to remove excess CO_2 from the surface. Finally, the desorption of CO_2 is performed by heating the sample from 50°C to 1000 °C, at a heating rate of 10°C/min under a pure flow of helium (20 mL/min). The dehydrogenation / dehydration of 2-propanol was carried out on a fixed-bed U-shaped Pyrex reactor and studied in the temperature range 175 to 250 °C, at atmospheric pressure using a 0.25% (v / v%) mixture of 2-propanol in helium (Air liquid) with a GHSV of 1007mL/g_{cat}.h.The reactor outlet gas composition was analyzed online by gas chromatography using an Agilent 7280D chromatograph equipped with a flame ionization detector (FID) and a capillary column HP_PLOT_U, L = 30 m, ID = 0.32 mm. Relative basicity was defined as the ratio between the selectivity to acetone (basic sites) and propene (acid sites), $\nu A / \nu P$.

2.2 *Catalytic measurements*

CO_2 methanation catalytic tests were carried out in a fixed-bed U-shaped Pyrex reactor with an internal volume of ≈7 mL. Mass flow controllers were used to control CO_2, H_2 and He flows. A gaseous mixture of CO_2 / H_2 (1:4 mol/mol) was used and the reaction studied with an adequate Gas Hourly Space Velocity (GHSV, 15000 mL of CO_2/g_{cat}.h). All tests were performed at atmospheric pressure and at a

range of temperatures 250 to 450 ºC. The catalysts were also submitted to a pre-treatment under hydrogen (10% H_2 in He). The reactor outlet gas composition was analysed online by a gas chromatography system using an Agilent 4890D GC equipped with a thermal conductivity detector (TCD). GC system uses a 6-port gas-sampling valve with a 0.250 mL loop. Catalyst activity was defined as the volume of CO_2 converted per g of catalyst per hour ($mLCO_2.g^{-1}.h^{-1}$). The values reported represent the steady state activities after 1 hour on stream. The conversion of CO_2 and selectivity to CH_4 and CO were calculated as follows: Conv. CO_2(%)= ($[CH_4]o+[CO]o$)/$[CO]o+[CH_4]o+[CO_2]o$)×100; Sel. CH_4 (%) = $[CH_4]o$/($[CO]o+[CH_4]o$)×100; Sel.CO (%) = $[CO]o$/($[CO]o+[CH_4]o$)×100, where $[CO_2]o$, $[CO]o$ and $[CH_4]o$ are outlet flow rates of CO_2 , CO and CH_4. Detector calibration was performed using external reference mixtures containing all reagents (CO_2, H_2) and expected products (CH_4, C_2H_4, C_2H_6, CO). The confidence level was better than 95%.

3 Results and discussion

3.1 *Catalysts characterization*

SEM images of the bimetallic cobalt – lanthanide oxides shows that the morphology of the samples is sensitive to the calcination temperature. In the case of the catalyst calcined at 450 °C its structure is spongier composed of very irregular spherical shape particles while, if calcined at 900 °C it is composed of a regular spherical shape nanoparticles agglomerates with an average size <100 nm (Figure 1).

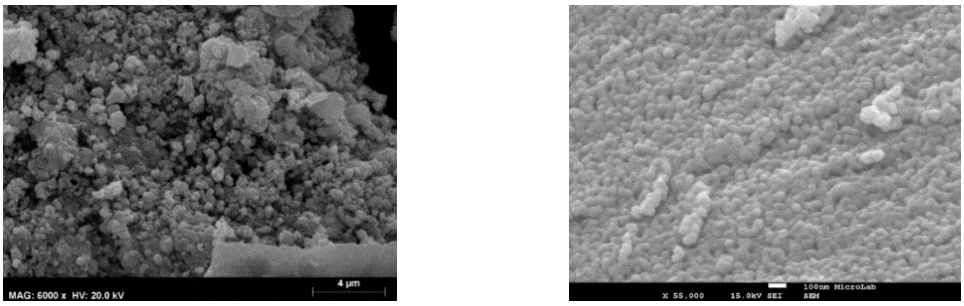

(a) (b)

Figure 1 – SEM images of bimetallic Co-Ln oxides: (a) Co-La oxide calcined at 450 ºC (x6000); (b) Co-Dy calcined at 900 ºC (x55000).

The EDS analysis at different points of the sample concluded that the elements are well distributed and that the cobalt / lanthanide ratio is close to expected (1: 1), with the surface mass percentage of Co approximately 20 to 25% for all catalysts. SEM images presented in Figure 1 are representative of the morphology of the remaining catalysts.

XRD patterns show that bimetallic cobalt-lanthanide oxides calcined at 450 ºC are quite amorphous but is possible to identify the cubic phase of cobalt oxide (Co_3O_4) in most cases (Figure 2a). Relatively to the *f*-block element phases, CeO_2 was observed in the Co-Ce catalyst, and for the remaining catalysts the tetragonal phase of lanthanide oxychloride (LnOCl; Ln = La, Sm, Gd, Dy) was identified, except of dysprosium and ytterbium. Oxychloride formation was also expected since it is known that for lanthanides, particularly those from the beginning of the series oxychlorides can be formed, when chloride salts are used in the preparation of the catalysts[13]. For bimetallic oxides calcined at 900 ºC (Figure 2b), the perovskite ($LnCoO_3$) phase is observed for all catalysts except for cerium and ytterbium,

since the latter requires temperatures above 1100^{0}C [14]. In these cases, the cubic phase of CeO_2 and Yb_2O_3 were formed with the cobalt oxide phase (Co_3O_4).

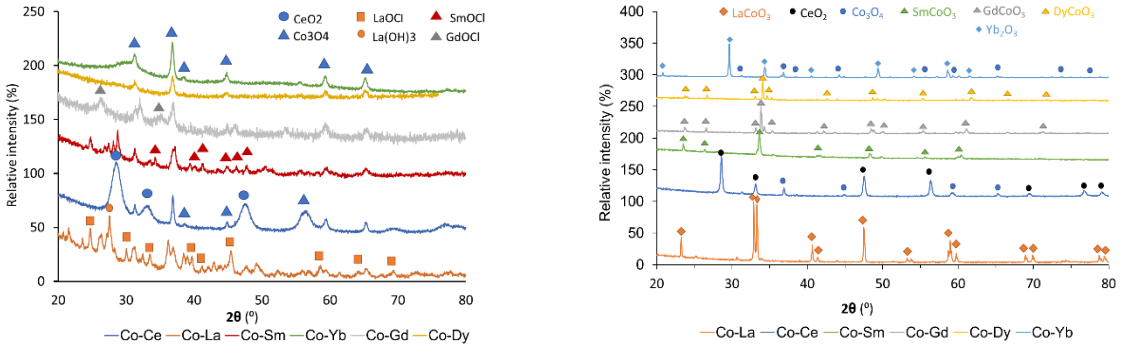

(a) (b)

Figure 2 - X-ray diffraction patterns of the bimetallic Co-Ln oxides calcined (a) at 450 ° C; (b) at 900 ºC.

The X-ray diffraction patterns obtained after catalytic studies with samples calcined at 450 ºC show that in the case of cerium and samarium catalyst there is a partial reduction of Co_3O_4 to CoO, while in the case of lanthanum catalyst the presence of metallic cobalt was also confirmed, indicating total reduction of Co_3O_4 to Co (Figure 3a). It should be noted that due to the maximum temperature tested for the CO_2 methanation reaction (450 ° C) both cerium oxide (CeO_2) and oxychlorides are stable under catalytic studies conditions. In the case of catalysts calcined at 900 ºC, it was verified that after reaction the total reduction of the Co_3O_4 phase to metallic cobalt was only observed for the Co-Yb catalyst. However, it was confirmed that either after reaction or for the pre-reduced samples the rare earth-containing oxide phase evolved from the perovskite phase to the sesquioxide phase (Figure 3b).

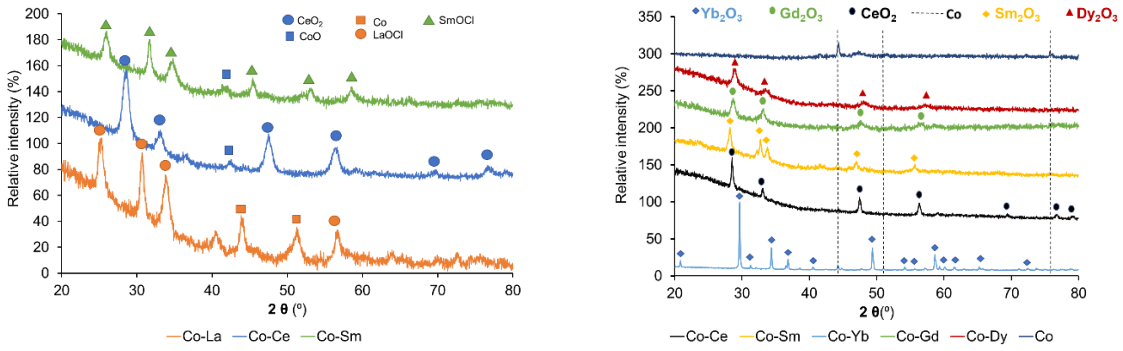

(a) (b)

Figure 3 - X-ray diffraction patterns obtained after reaction for the bimetallic oxides calcined (a) at 450 ° C; (b) at 900ºC.

The H_2-TPR results show that each lanthanide has an effective influence on the catalysts oxygen's reducibility / lability. In all cases, either for the catalysts obtained after calcination at 450 ºC or for those obtained after calcination at 900 ºC, the main reduction steps occurs at temperatures well above the reduction temperature obtained for the monometallic Co catalyst prepared in the same conditions and calcined at 450 and 900 ºC, 334 and 378 ºC, respectively (Figure 4).

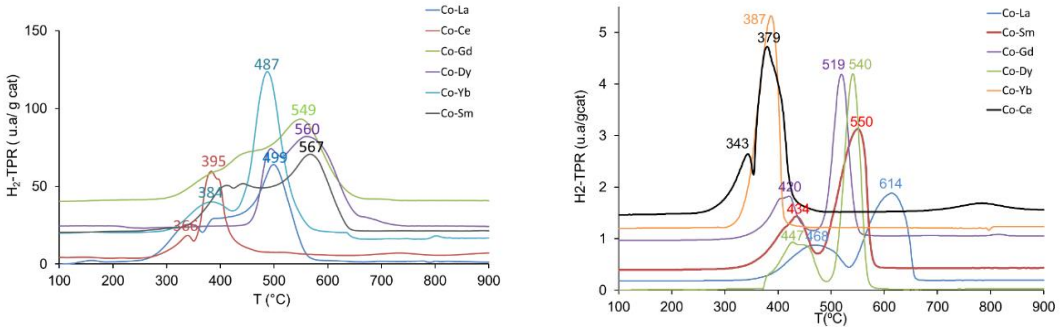

Figure 4 - H_2-TPR profiles for bimetallic cobalt-lanthanide oxides calcined (a) at 450 ºC (b) at 900 ºC.

For the catalysts calcined at 450 ºC, where oxychloride is present (La, Sm, Gd, Dy) the profiles are complex and composed of several reduction steps that are not delimited by well-defined peaks (Eq. 1-2). In the case of ytterbium and cerium the profiles show that the reduction of Co_3O_4 occurs in two well-defined peaks (Eq.3-4). The bimetallic oxide catalysts calcined at 900°C display also a two-step reduction profile associated in a first step with the reduction of $LnCoO_3$ to Ln_2O_3.CoO and, in a second step, the reduction of CoO to metallic Co (Eq. 5-6).

$$3LnOCl.Co_3O_4 + H_2 \rightarrow 3LnOCl.3CoO + H_2O \quad (1)$$
$$3LnOCl.3CoO + 3H_2 \rightarrow 3LnOCl.3Co + 3H_2O \quad (2)$$
$$Co_3O_4 + H_2 \rightarrow 3CoO + H_2O \quad (3)$$
$$3CoO + 3H_2 \rightarrow 3Co + 3H_2O \quad (4)$$
$$2LnCoO_3 + H_2 \rightarrow Ln_2O_3.2CoO + H_2O \quad (5)$$
$$Ln_2O_3.2CoO + 2H_2 \rightarrow Ln_2O_3.2Co + 2H_2O \quad (6)$$

Table 2 - Theoretical and experimental values obtained for hydrogen consumption using the catalysts calcined at 450 ° C.

Catalyst	*Uptake H_2(µmoles)*	Theoretical moles	Exp./Theor.ratio	Tm (º C)
Co_3O_4	79.5	84.7	0.94	334.7
Co_3O_4.3LaOCl	151.2	176.0	0.87	449.1
Co_3O_4.3CeO_2	115.0	183.1	0.62	395.7
Co_3O_4.3SmOCl	159.5	183.7	0.87	567.3
Co_3O_4.3GdOCl	143.7	151.1	0.95	549.5
Co_3O_4.3DyOCl	77.7	90.2	0.86	560.4
2Co_3O_4.3Yb_2O_3	174.4	212.2	0.82	487.6

Table 3 - Theoretical and experimental values obtained for hydrogen consumption using the catalysts calcined at 900 ° C.

Catalyst	*Uptake H_2(µmoles)*	Theoretical moles	Exp./Theor.ratio	Tm(ºC)
Co_3O_4	17.6	18.3	0.96	378.0
$LaCoO_3$	100.2	112.3	0.89	613.8
Co_3O_4.3CeO_2	110.2	119.7	0.92	379.5
$SmCoO_3$	116.1	118.3	0.98	550.1
$GdCoO_3$	84.7	89.8	0.96	519.2
$DyCoO_3$	109.1	112.5	0.99	540.5
2Co_3O_4.3Yb_2O_3	87.1	88.9	0.98	386.9

Also, noteworthy the good agreement between the theoretical and actual values obtained for hydrogen consumption (Table 2 and 3), which seems to confirm the reducibility profiles just described .

The catalysts acid-base properties were studied by CO_2-TPD and studying the dehydrogenation/dehydration of 2-propanol as model reaction. The results obtained by the two techniques show a good agreement and a good correlation between them (Figure 5).

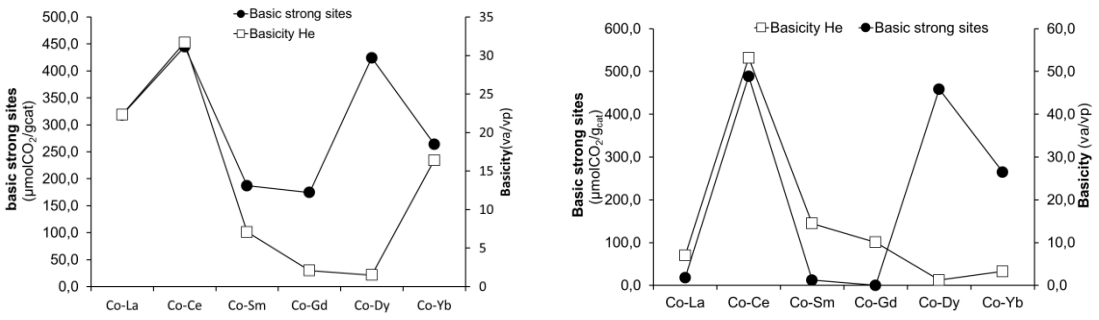

(a) (b)

Figure 5 - Acid-base properties of bimetallic cobalt-lanthanide oxides (strong basic sites, CO_2-TPD; va/vp, dehydrogenation/dehydration of 2-propanol in inert atmosphere at 250 ºC calcined at 450 ºC (a); at 900 ºC (b).

3.2 *CO_2 Hydrogenation*

The type of preparation effect was studied over two samples of cobalt-cerium bimetallic oxides obtained by two different approaches of the sol-gel method: the epoxide addition method and the Pechini method. Figure 6 shows that the results obtained with the sample prepared by the epoxide addition method are clearly better than those of the sample prepared by the Pechini method. Therefore, the epoxide addition approach was chosen for the preparation of all remain catalysts.

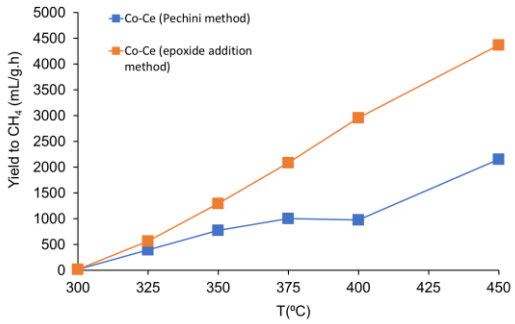

Figure 6 - Effect of synthesis method on the yield to CH_4 of the cobalt-cerium catalyst (H_2/CO_2=4, GHSV=15000 mL CO_2 / gcat.h).

The positive effect subsequent to the addition of rare earth to cobalt catalysts was also confirmed by comparing the results obtained with pure metal oxides of cobalt and cerium with those of the cobalt-cerium bimetallic oxide obtained by the epoxide addition method (Figure 7). Under the same conditions, pure cerium oxide has no catalytic activity whereas the activity of the monometallic Co catalyst is substantially improved by the addition of cerium.

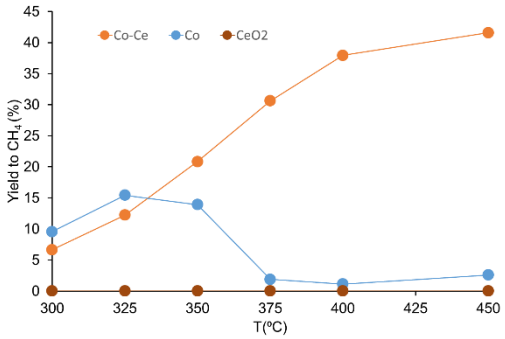

Figure 7 – Comparison of yields to CH_4 between pure metal oxides of cobalt, cerium and bimetallic cobalt-cerium catalyst (H_2/CO_2=4, GHSV=15000 mL CO_2 / g_{cat}.h)

The calcination temperature employed in the last catalyst preparation step plays also a decisive role in the type of oxide phases obtained and consequently influences the nature of the active species for the carbon dioxide hydrogenation. The results show that catalysts calcined at 900 ºC in general are more active, but less selective to CH_4 with and without pre-reduction under hydrogen (not shown). (Figure 8)

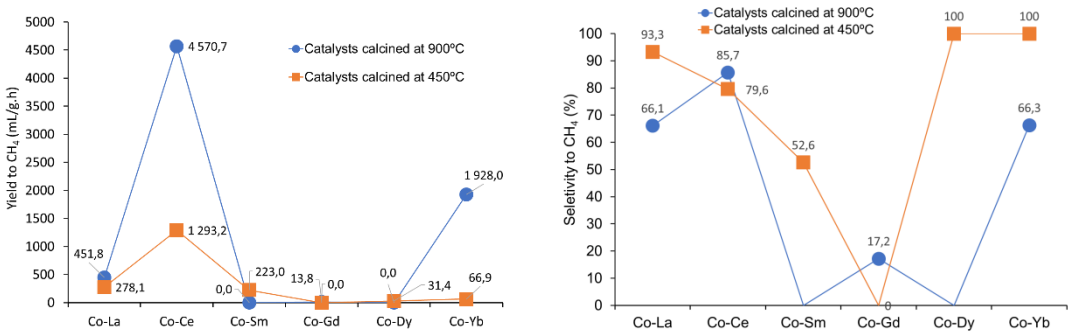

(a) (b)

Figure 8 – Influence of the calcination temperature of catalysts on the: yield to CH_4 (a); selectivity to CH_4 (b) (H_2/CO_2=4, GHSV=15000 mL CO_2 / gcat.h, reaction temperature=350 ºC).

The effect of the pre-reduction treatment of the catalysts prior to their test on the CO_2 methanation was also studied. This step is mentioned in the literature as indispensable for the formation of the dominant active species, in this case, the metallic cobalt. The results obtained shows that, in almost all cases, the pre-reduction of the catalysts obtained after calcination at 450 and 900 ºC has a positive effect on the catalysts activity, except for the Co-Sm catalysts obtained after calcination at 450 ºC and the Co-La catalyst obtained after calcination at 900 ºC. In particular, the behavior of Co-La catalyst can be explained by the fact that its pre-reduction requires a very high temperature (700 ºC), which leads to an increase in particle size (sintering) and loss of active surface area due to sample sintering [15,16]

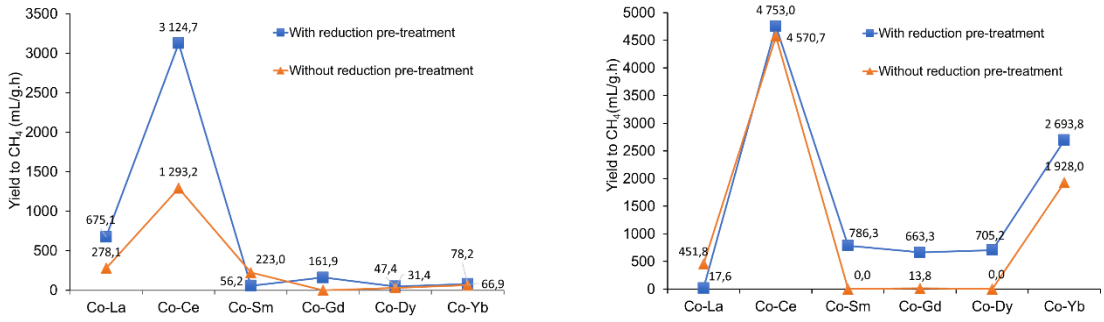

(a) (b)

Figure 9 - Pre-treatment effect on the activity of the catalysts calcined at 450 ºC (a); at 900 ºC (b). (H_2/CO_2=4, GHSV=15000 mL CO_2 / gcat.h, reaction temperature=350 ºC)

Figure 10 shows, as an example, the results obtained over the Co-Ce catalyst obtained after calcination at 900 ºC. The catalyst is stable for at least 10 hours at each temperature studied, except at 450 ° C. It is known that cobalt based catalysts are a relatively resistant to thermal deactivation. Nevertheless, cobalt catalysts often suffer carbon deposition, changes in porosity and surface morphology and, in some cases, crystalline phase transformation may also occur, namely by reoxidation of cobalt particles leading to its deactivation [17,18].

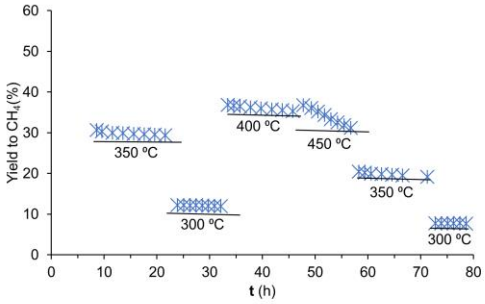

Figure 10 - Stability of the bimetallic Co-Ce catalyst calcined at 900 ºC with pre-reduction (H_2/CO_2=4, GHSV=15000 mL CO_2 / gcat.h)

Finally, we have studied the rare earth influence along the lanthanide series on the catalysts activity and selectivity. For this purpose, a comparison was made between the catalytic activity and the intrinsic properties of bimetallic oxides catalysts, as the acid-base properties are known to directly influence the catalysts behavior [19]. The results show that regardless of the calcination temperature, the yield of methane increases with the basicity (Figure 11). The cobalt - cerium catalyst is clearly the most active.

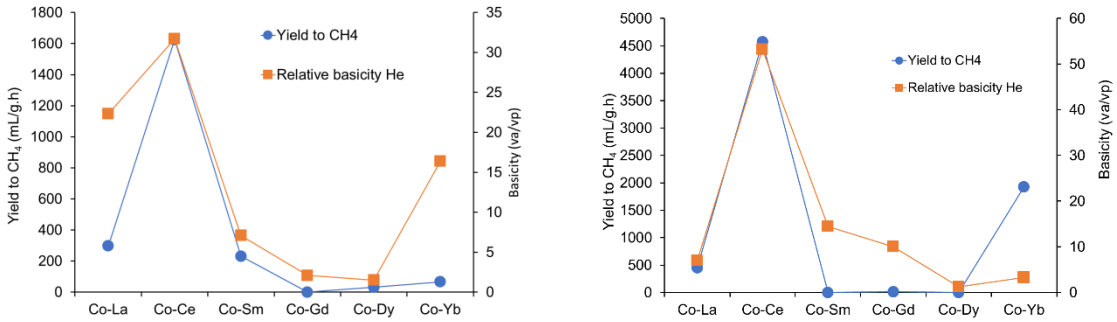

(a) (b)

Figure 11 – Influence of relative basicity on the catalytic behavior of the bimetallic cobalt-lanthanide oxides calcined (a) at 450 ºC; (b) at 900 ºC.

As for the reduction properties, it was also observed that there is also an inverse correlation between catalyst activity and the controlled atmosphere reduction temperature for both the type of samples: calcined at 450 ºC or calcined at 900 ºC, with and without reduction (Figure 12). It is thus obvious that the presence of rare earth is not merely figurative and that there is a synergy between metals that explain the enhanced activity of cobalt after the addition of rare earths.

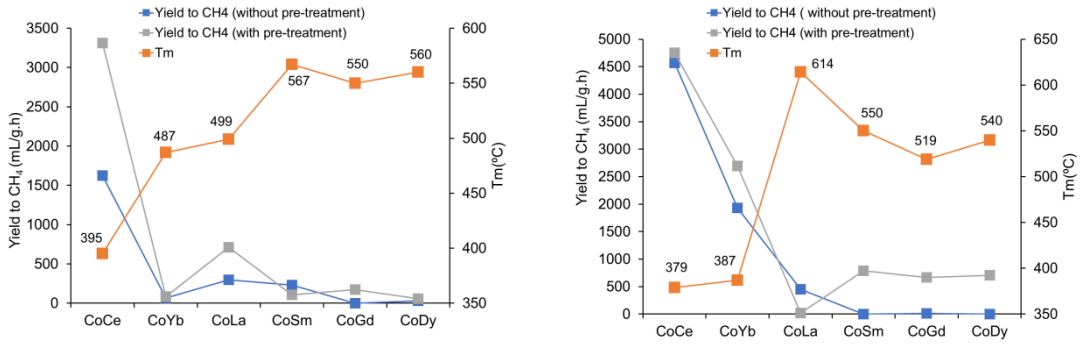

(a) (b)

Figure 12 – Influence of reduction temperature in catalytic activity of bimetallic cobalt-lanthanide oxides calcined (a) at 450 ºC; (b) at 900 ºC.

4 Conclusion

The study of bimetallic Co-Ln oxides (Ln=La, Ce, Sm, Gd, Dy and Yb; Co/Ln=1) as catalysts for CO_2 hydrogenation was undertaken. The aerogels were obtained by the epoxide addition method (sol-gel method), which demonstrated to be better when compared to the Pechini method. As intended, the samples had high specific areas (> 100 m^2 / g).The calcination of aerogels at different temperatures, 450 ºC and 900 ºC, led to the formation of distinct oxide phases: oxychlorides in the case of calcination at 450 ° C (Co_3O_4.3LnOCl; Ln = La, Sm, Gd and Dy) and perovskites in the case of calcination at 900 °C ($LnCoO_3$; Ln = La, Sm, Gd and Dy). In both cases, the exceptions were the Co-Ce and the Co-Yb catalysts that stabilize as sesquioxides, Co_3O_4.3CeO_2 or 2Co_3O_4.3Yb_2O_3, respectively. Evidence of the existence of a synergistic effect between the two metals (Co and Ln) was found from their behavior under reducing atmosphere (H_2-TPR).

Regarding their catalytic performance, the best results were obtained with the bimetallic Co-Ce oxide catalyst at 900 ºC (CO_2 conversion = 37%, selectivity in CH_4 = 85.7%). The main factors that seem to contribute to the variation of catalyst activity and selectivity are their acid-base properties and reducibility of oxide phases. The activity and the selectivity increase with catalysts basicity, showing an inverse dependence of the reduction temperature.

In conclusion, the reuse of CO_2 as a raw material for the formation of value-added products is one of the most attractive prospects today, despite the need for continued research to make this process an increasingly viable industrial alternative.

5 References

[1] W. Li, H. Wang, X. Jiang, J. Zhu, Z. Liu, X. Guo, C. Song, *RSC Adv.* **2018**, *8*, 7651–7669.
[2] E. S. Sanz-Pérez, C. R. Murdock, S. A. Didas, C. W. Jones, *Chem. Rev.* **2016**, *116*, 11840–11876.
[3] M. Bui, C. S. Adjiman, A. Bardow, E. J. Anthony, A. Boston, S. Brown, P. S. Fennell, S. Fuss, A. Galindo, L. A. Hackett, et al., *Energy Environ. Sci.* **2018**, *11*, 1062–1176.
[4] P. Frontera, A. Macario, M. Ferraro, P. L. Antonucci, *Catalysts* **2017**, *7*, 1–28.
[5] J. Zheng, C. Wang, W. Chu, Y. Zhou, K. Köhler, *ChemistrySelect* **2016**, *1*, 3197–3203.
[6] T. Riedel, M. Claeys, H. Schulz, G. Schaub, S.-S. Nam, K.-W. Jun, M.-J. Choi, G. Kishan, K.-W. Lee, *Appl. Catal. A Gen.* **1999**, *186*, 201–213.
[7] R. W. Dorner, D. R. Hardy, F. W. Williams, B. H. Davis, H. D. Willauer, *Energy and Fuels* **2009**, *23*, 4190–4195.
[8] J. Zhang, X. Su, X. Wang, Q. Ma, S. Fan, T. S. Zhao, *React. Kinet. Mech. Catal.* **2018**, *124*, 575–585.
[9] S. Zeng, Y. Du, H. Su, Y. Zhang, *CATCOM* **2011**, *13*, 6–9.
[10] T. A. Le, M. S. Kim, S. H. Lee, E. D. Park, *Top. Catal.* **2017**, *60*, 714–720.
[11] A. Kumar, A. Rana, G. Sharma, S. Sharma, M. Naushad, G. Tessema, *Environ. Chem. Lett.* **2018**, *16*, 797–820.
[12] S. G. Rudisill, N. M. Hein, D. Terzic, A. Stein, *Chem. Mater.* **2013**, *25*, 745–753.
[13] B. J. Clapsaddle, B. Neumann, A. Wittstock, D. W. Sprehn, A. E. Gash, J. H. Satcher, R. L. Simpson, M. Bäumer, *J. Sol-Gel Sci. Technol.* **2012**, *64*, 381–389.
[14] L. Ben Farhat, R. Ben Hassen, L. Dammak, *Powder Diffr.* **2007**, *22*, 35–39.
[15] J. Xu, X. Su, H. Duan, B. Hou, Q. Lin, X. Liu, X. Pan, G. Pei, H. Geng, Y. Huang, et al., *J. Catal.* **2016**, *333*, 227–237.
[16] S. Tada, R. Kikuchi, K. Urasaki, S. Satokawa, *Appl. Catal. A Gen.* **2011**, *404*, 149–154.
[17] C. Ahn, H. Mo, M. Jin, J. Man, T. Kim, Y. Suh, K. June, J. Wook, *Microporous mesoporous Mater.* **2014**, *188*, 196–202.
[18] A. Y. Khodakov, W. Chu, P. Fongarland, **2007**, 1692–1744.
[19] K. Tanabe, *Solids Acids and Bases*, Academic Press, **1970**.